KSCE Journal of Civil Engineering (2019) 23(7):2933-2947

DOI 10.1007/s12205-019-0716-8

Structural Engineering

pISSN 1226-7988, eISSN 1976-3808
www.springer.com/12205

Optimal Sensor Placement of RCC Dams using Modified Approach of COMAC-TTFD

Hamidreza Vosoughifar* and Milad Khorani**

Received April 12, 2018/Revised October 24, 2018/Accepted February 18, 2019/Published Online May 27, 2019

Abstract

The optimal sensor placement is the most important issues for structures health monitoring (SHM) of RCC (roller-compacted concrete) dams. In past studies, the main achievement focus on optimal criterions of sensor locations were considered via modal test. In this study a novel approach based on modified coordinate of modal assurance criterion (COMAC) with transferring time history analysis results to frequency domain (TTFD) for the SHM of RCC dam was evaluated. The nonlinear time history analysis of RCC dam subjected to near and far field earthquake were considered in TTFD process. The FEMCRTTFD code in MATLAB was designed as a toolbox to perform all of process of this novel approach by authors of this paper. The validation process of this code has been done via comparing with the reference study. The comparison between sensors placement that calculated by COMAC and TTFD show that the modified method has good agreement and accurate placement of smart sensors. Statistical results show that there is no significant difference between the results of TTFD method and COMAC in cracked dam, except Manjil earthquake (the mean of p-value = 0.717). The results indicate that considering modified COMAC calculation based on TTFD approach has an acceptable accuracy on identify the sensor location.

Keywords: *health monitoring, RCC dam, optimal sensor placement (OSP), TTFD approach, modal analysis*

1. Introduction

The health of dam structures are affected by potential risks such as: floods, storms, landslides, internal erosion, improper design, maintenance and earthquakes. So the SHM (structures health monitoring) of dam structures during the operation period, is one of the most important issue. It is still rather impracticable to predict the mouth and depth of cracks or development of failure in concrete dam structures, which is important for the assessment of dam health in operation period. Recently to simulate seismic and smeared cracks various fracture mechanism models have been used. The seismic loads are the main cause of cracking in concrete gravity dam. Many studies has been done on the smeared cracks in seismic analysis. Saini and Krishna (1972) studied the stability of the Koyna dam with combination single and smeared cracks where occurred in place of the slope changes suddenly. Two classes of fracture models, namely, the discrete crack model (Rashid, 1968) and smeared crack model (Hillerborg *et al*., 1976) have been evaluated.

It is critical for dam safety assessment when dam is subjected to seismic waves. The non-linear analysis can be modeled the effect of seismic loads on dam using combination between different fracture mechanism models. A set of concrete micromechanical damage models were developed in the last decade such as: Random particle pattern (Bazant and Tabbara, 1990), lattice model (Schlangen and Garboczi, 1997), micromechanical model (Mohamed and Hansen, 1999). Harris *et al.* (2000) researched on the method of crack incidence using the experimental method with various seismic waves that produced by verified shaking table. Tang and Zhu (2003) developed the Harris *et al.* (2000) research based on random mechanical characteristic model. Javanmardi *et al.* (2005) considered a novel fracture model for predication seismic cracks with considering static and dynamic water pressure. Zhu and Pekau (2007) evaluated all active modes for developing concrete cracks beside their impacts on the stability of concrete gravity dam. Zhang *et al.* (2009) studied on two different types of discrete cracks using seismic finite element analysis. Most of the micromechanical damage models, due to the limited computing capacity, were only used for the numerical simulation of a single concrete member. These methods cannot be used to analyze the very small damage and macro cracking of the entire concrete dams, or another intricate concrete structure (Huang *et al*., 2008). The random mechanical characteristic model, which considers the influence of inhomogeneity in the micro views on the basis of macroscopic homogeneity assumption, is a proper method for simulating the seismic crack of concrete dam

*Assistance Professor, Dept. of Civil Engineering, Islamic Azad University, Tehran South Branch, Tehran, Iran; Research Scholar, Dept. of Civil and Environment Engineering, Hawaii University at Mano, Honolulu 96822, USA (Corresponding Author, E-mail: vosoughifar@azad.ac.ir; vosoughi@hawaii.edu)
**M.Sc. Student, Dept. of Civil Engineering, Islamic Azad University, Tehran South Branch, Tehran, Iran (E-mail: miladkhorani@gmail.com)

structure. But it is not feasible to analyze the damage and cracking of concrete dams in a large scale. The ultimate failure patterns that measured with this method were consistent with the ones obtained from laboratory tests for the seismic damage analysis of a dam (Zhong *et al*., 2009). The classical fracture mechanics cannot define the production of initial micro cracks. Nonetheless, the proper fracture mechanism may be of use to discuss the evolution process of the mechanical attributes of concrete dams from micro crack initiation to final defeat under the effect of seismic loads (Xiong *et al*., 2014). The fracture mechanism with production of initial micro cracks was evaluated the deformation and stress of concrete dams (Wang *et al*., 2017). Hariri-Ardebili and Seyed-Kolbadi (2015) via estimating the dam cracking capacity and modeling of material behavior proposed a model for the instability of concrete dams and seismic cracks. Wang *et al*. (2017) evaluated a three dimensional nonlinear finite element analyses for Guandi concrete dam. They determined Seismic damage in this dam.

The importance of crack monitoring is determining the appropriate time to repair damage in structure. Fiber optic sensors network was considered as a modern technique for SHM of concrete dams. These systems are suitable for SHM and also the cracks control. A network of smart sensors can be used based with fiber optic network for online crack monitoring of concrete gravity dams in the course of service loads. Hemez and Farhat (1994) evaluated a new algorithm that expanded the effective endurance method by optimizing the sensors placement in terms of structural energy contributions. Shi *et al*. (2000) studied the optimal sensors placement for damage detection in structures. Hiramoto *et al*. (2000) provided a new method for determining the optimal placement of sensors and vibrations control based on the explicit equation. Wouwer *et al*. (2000) proposed a pattern for selecting optimal sensor locations. This criterion is developed based on the assessment on the independence of sensor responses. Worden and Burrows (2001) used various methods to determine the location and optimal distribution of sensors based on curvature data. Guo *et al*. (2004) optimized the location of the sensors using the genetic algorithm that can made convergence in analysis process to get the exact results faster.

Shokouhi *et al*. (2013) proposed a new method based on TTFD (transformed time history to frequency doman) approach using genetic algorithm and finite element method to optimize sensors placement in the base-isolated structures. Vosoughifar *et al*. (2012) analyzed an UBF (unbonded braced frame) steel structure and optimized sensors placement by using the novel genetic algorithm. Vosoughifar and Shokouhi (2013) evaluated a novel optimization method to find optimal placement of smart sensors in LSF (lightweight steel frame) structure. In this study, the seismic response was determined using the TTFD approach and the optimum location for the sensors was determined using the genetic algorithm (GA) with multi-objective target. Moradi *et al.* (2014) identified the locations of sensors where the cavitation occur in underground storage tanks with using the Monte-Carlo analysis. They suggested the best location for the installation of smart sensors through the same analysis. Zhao *et al*. (2015) discussed a new fiber optic sensor that they can sense small cracks in isotropic homogeneous materials. Ju *et al*. (2015) suggested some strategies for structural health monitoring of cable supported bridge with sensors. Rathi and Gupta (2016) used the new approach of genetic algorithm (GA) to determine the sensor location in water distribution network. In this research, a proper fracture mechanism was used for focusing on anticipating the damage and cracking characteristics of concrete dams. This case study were subjected to earthquakes with various intensities. The Zirdan dam in Iranshahr in Iran that is a RCC (roller-compacted concrete) dam was selected as case study in this research. The novel approach analysis in this research is verified by the same results of the Koyna dam. The aim of this study is define a novel OSP (optimal sensor placement) approach based on COMAC (coordinate of modal assurance criterion) to consider the seismic behavior of concrete dam subjected to near and far field earthquakes. In this respect the frequency domain was used to transfer the actual seismic behavior of dam with considering seismic loads and crack consideration to behavior same as modal analysis. The results of this analysis can be used on OSP for health monitoring of concrete dams. The novel approach was called FEMCRTTFD with unique ability to make an integration between nonlinear FE (finite element) analysis and optimization process of OSP.

2. Fracture Mechanism of FEMCRTTFD

The suggested model can simulate the behavior of concrete in various states including pre-softening behavior; nonlinear behavior during the softening step; and finally, crack opening and reclosing behavior. In the pre-softening step, supposedly there is a linearly springy relation between both the tenseness and genuflection vectors. Orthotropic, isotropic, and an-isotropic materials can be defined by elastic modulus matrix$[U]_{el}$. During the softening step, the elastic stress–strain relationship is substituted with an isotropic modulus matrix. A proper module is applied in this research to get the toughness effect. The toughness module based on the molten propagation of crack is given in Eq. (1). The principal strains in the given position and the derived matrix of modulus can model non-linear within the cracked element:

$$[U]_{cr}^{L}=\begin{bmatrix} \frac{\delta_1 E(1-v^2\delta_2\delta_3)}{\psi} & & & & & \\ \frac{v\delta_1\delta_2 E(1+v\delta_3)}{\psi} & \frac{\delta_2 E(1-v^2\delta_1\delta_3)}{\psi} & & & & \\ \frac{v\delta_1\delta_3 E(1+v\delta_2)}{\psi} & \frac{v\delta_2\delta_3 E(1+v\delta_1)}{\psi} & \frac{\delta_3 E(1-v^2\delta_1\delta_2)}{\psi} & & & \\ 0 & 0 & 0 & \alpha_{12}\tau & & \\ 0 & 0 & 0 & 0 & \alpha_{23}\tau & \\ 0 & 0 & 0 & 0 & 0 & \alpha_{12}\tau \end{bmatrix} \quad (1)$$

where δ_1, δ_2 and δ_3 are the ratios of the softened Young's

modulus in the three main directions and the initial isotropic elastic modulus, respectively.

α_{12}, α_{23}, α_{23}, and α_{13} are shear transfer coefficients corresponding to the principal directions and τ is the shear modulus. The value of ψ is given by Eq. (2):

$$\psi = 1 - v^2\delta_1\delta_2 - v^2\delta_2\varepsilon_3 - v^2\delta_1\delta_3 - 2\delta^2 v_1 v_2 v_3 \tag{2}$$

The softened shear modulus corresponding to $i-j$ axes on the fracture plane can be elaborated by the principal stresses and the shear transfer coefficients. This values can be obtained as Eq. (3):

$$\begin{cases} \alpha_{12} = \dfrac{1+v}{\psi}\left(\dfrac{\delta_1\varepsilon_1 - \delta_2\varepsilon_2 - v\delta_3(\delta_1-\delta_2)\varepsilon_3}{\varepsilon_1-\varepsilon_2} - v\delta_1\delta_2 - 2v^2\delta_1\delta_2\delta_3\right. \\ \alpha_{23} = \dfrac{1+v}{\psi}\left(\dfrac{\delta_2\varepsilon_2 - \delta_3\varepsilon_3 - v\delta_1(\delta_2-\delta_3)\varepsilon_1}{\varepsilon_1-\varepsilon_2} - v\delta_2\delta_3 - 2v^2\delta_1\delta_2\delta_3\right. \\ \alpha_{13} = \dfrac{1+v}{\psi}\left(\dfrac{\delta_1\varepsilon_1 - \delta_3\varepsilon_3 - v\delta_2(\delta_1-\delta_3)\varepsilon_2}{\varepsilon_1-\varepsilon_3} - v\delta_1\delta_3 - 2v^2\delta_1\delta_2\delta_3\right. \end{cases} \tag{3}$$

The constitutive matrix ($[U]_{cr}^{L}$) that given in Eq. (1) convert to universal peculiarities set ($[U]_{cr}^{G}$) with using the strain transformation matrix ([T]). According to the maximum strain available in each main direction, the secant modulus matrix can be determined. If the normal toughness enhances in each main trend, the corresponding softened Young's module will reduce. Finally, with the maximum strain in the fracture, the given Gaussian point in cracked element and its contribution in the toughness matrix was eliminated. According to Eqs. (1) and (2), if the main strains or their trends change in each Gaussian point, the universal fundamental matrix ($[U]_{cr}^{G}$) will be essential to apply. The shear transfer coefficient (a) contributes to shear transfer among sheet of a tensile crack when the crack is opened or closed. In the given model, the concrete is cracked in three perpendicular trends to each other. All the parameters are updated by a spin crack model in each load phase. The shear transition coefficients are influenced in two other trends and can be calculated by the cracked Gaussian point model in one trend. Otherwise, the behavior of that cannot evaluated by constant crack model. In this case, the softened local module is shown as Eq. (2), while only the three last arrays on the diagonal of this matrix are different (U_{cr44}^{L}, U_{cr55}^{L}, and U_{cr66}^{L}). Hereon, two constant shear transition coefficients are applied instead of the variable ones and can model the cracked Gaussian point in natural trend. The crack condition such as opened mouth (α_O) or closed mouth (α_C,) are used as the shear transition coefficients. Fig. 1 shows the strain versus compressive stress in laboratory test for both cements that used in the dam structure.

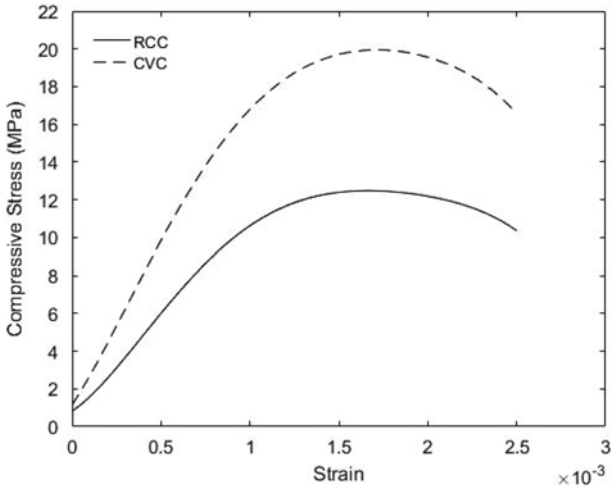

Fig. 1. Comparison between of the Stress–Strain Curve for RCC and CVC Concrete

2.1 Lagrangian FE Method for Dam-Reservoir System

The relation for the FE analysis depends on Lagrangian approach for interaction between fluid-solid systems was considered in FEMCRTTFD. The evacuations were selected to be the unknown variables for both the fluid and structure domains. It is assumed that the fluid has non-compressible, resilient, and adhesive property. The stress-strain relation in three-dimensional element can be defined by Eq. (4):

$$\begin{Bmatrix} P \\ P_x \\ P_y \\ P_z \end{Bmatrix} = \begin{bmatrix} C_{11} & 0 & 0 & 0 \\ 0 & C_{12} & 0 & 0 \\ 0 & 0 & C_{33} & 0 \\ 0 & 0 & 0 & C_{44} \end{bmatrix} \begin{Bmatrix} \varepsilon_v \\ Q_x \\ Q_y \\ Q_z \end{Bmatrix} \tag{4}$$

where P is the pressure, C_{11} is the compressive modulus of fluid, ε_v is the volumetric strain. Q_y and Q_z are the rotations depending on the Cartesian axis x, y, z, respectively. P_x, P_y, and P_z are the corresponding rotational stresses. C_{22}, C_{33}, and C_{44} are the constraint parameters depending fluid property. The irrotational property of fluid can be defined by setting the finite element parameters in the tension-toughness criteria. In this research the effect of the small waves in the water surface generally called as the sloshing effect, was considered. The free surface of fluid is compressed by fortissimo effect, which is given by Eq. (5):

$$P = -\gamma_f u_n \tag{5}$$

where γ_f is the weight density of fluid and u_n is the normal component of the free surface displacement. The discrete form of Eq. (5) evaluates any toughness in free surface of fluid.

3. Methodology

The main purpose of evaluating a novel approach for health monitoring of concrete dams is to develop the existing COMAC criteria with worthier computational process and make more reliable method in this issue. This criterion was carried out using the modal and seismic time history analysis to make modified type of COMAC method and estimate the optimal sensor placement. The tensile potential of concrete in dam body was considered as one of research limitation to detect the wake points in dam. The tensile cracks was considered as potential failure of dam so the cracking initiation and amount of growth crack are very important in designing proper nonlinear FE. The stable

section of dam was used as case study therefore the deformation and sliding limit were not considered in this criteria, however they can be used in the future criteria. A new method called transformed time history to frequency domain (TTFD) was evaluated to transform time history analysis results to frequency domain. Because the concrete gravity dam has effective natural modes, the modified MAC and COMAC values of the seismic waves corresponding each level were calculated. The frequency-domain obtained with the FEMCRTTFD criteria was used to analysis the near and far field seismic waves in OSP process. This approach can consider the actual earthquake waves on MAC (modal assurance criterion) and COMAC algorithm. The basic idea apply to generate frequency amplitude from seismic displacement of dam in selected levels of dam. The deconvolved motion was estimated based on the integrated form solution of near and far field waves. The selected concrete gravity dam was modeled into FEM-COMAC with their equivalent properties (i.e., density (ρ), module of elasticity (E), damping (ζ), shear module (G)). The finite element used directly to deconvolve the seismic near and far field ground motions. The near field analysis was modeled subjected to bidirectional excitation waves. Then, the relationship between time history analysis and modified COMAC can be expressed in frequency domain in term of function like: Amplitude and phase shift. The amplitude and phase of input earthquake and convolved waves can be expressed by Fourier transform so it can be used to determine the deconvolved displacement in frequency domain. The seismic behavior of concrete gravity dam is different for motion into the U/S or D/S directions. Therefore, there is various COMAC values in both opposite directions.

The modal behavior of dam and displacement of dam from base to crest belong to the main frequencies of time history analysis were used as the main variable in calculation of modified COMAC amount. The crest displacement is also controlled in time history analysis which is employed to make a limitation parameter in optimization process.

The main advantage of FEMCRTTFD approach is its accuracy and simplicity. Structural behavior of body dam can be obtained from a simple nonlinear FE model. There are some obscurities, for example, how much sensors are necessary to detection damage in dam body and what is the acceptable level of COMAC value to optimize sensors placement. This novel approach can reduce computational process and collect all of OSP process in one criteria. In spite of assumption and simplification, this methodology can detect the sensor placement from nonlinear seismic analysis. The proposed methodology can optimize the number and placement of sensors for health monitoring of dam subjected to seismic loads. The FEMCRTTFD can optimize the sensor location to detect damage after a natural disaster like earthquake. The fitness function, multi-objective and limitation of Fiber Bragg Gratings (FBGs) sensors must be defined in optimization process. Light traveling of the optical fiber sensors can detect displacement, strain or temperature. This sensor consist three layers include: The core, the cladding, and outer coating. The FBGs sensors can use to measure strain or displacement. The wire sensors can damage easily so the FBG can solve the complex wire problems and make sequential measurement. This characteristic of FBG makes it possible to make the on time measuring of large amount of data. However, the practical application of such sensors is limited due to their relatively high price. In strain applications, the maximum wavelength shift possible without breaking the sensor is about 4,000 micro stain which is a limitation to use FBG sensors. Therefore, with cost consideration the number of sensors and about maximum wavelength the distance of sensors must be limited in optimization process of FEMCRTTFD approach.

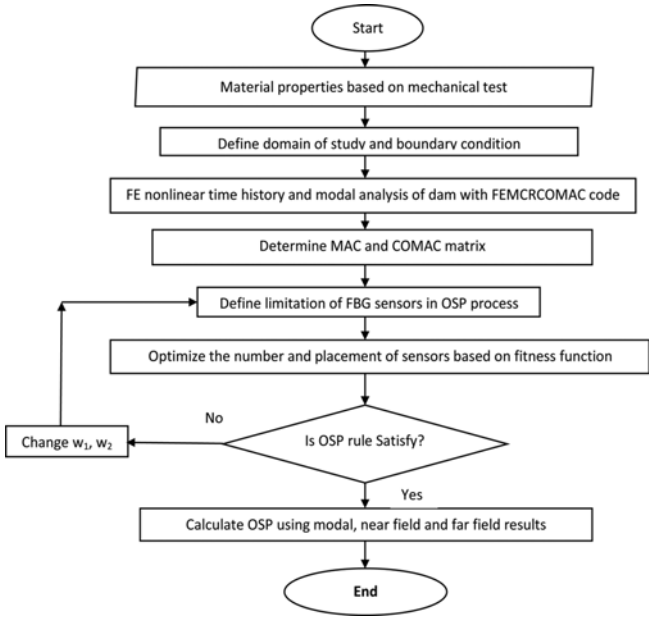

Fig. 2. Optimized Flowchart for the FEMCRTTFD Code

The applied approach in this code to solve a multi-objective optimization problem is to assign a proper weight to each normalized objective function. In this respect the problem is converted to a single objective problem with a scalar objective function. The fitness function of FEMCRTTFD approach is given by Eq. (6). The first part of this fitness function optimize the sensor placement and the second part of that optimize the number of FBGs sensors:

$$f = w_1(1-\sum_1^z(1-modified\ \ COMAC_h)) + w_2(cost) \quad (6)$$

where, $(1-\sum_1^z(1-modified\ \ COMAC_h))$ and cost are the normalized objective function, and sum of weights equals 1 ($\sum w_i = 1$). The main difficulty of using this method is selecting a weight vector for each run. The number and placement of sensor are very important in optimization process so in this study, the value of w_1 and w_2 change from 0.4 to 0.6. The flowchart of integrated methodology is explained step by step in Fig. 2.

4. Case Study

The Zirdan RCC dam was considered in this research as case

(a) (b)

Fig. 3. Zirdan Dam: (a) Layout and Position, (b) 3D View

Table 1. The Concrete is Assumed to Have the Following Basic Properties

ID	Material parameters	CVC concrete	RCC concrete
1	Compressive strength	Fc = 20 MPa	Fc=12.5 MPa
2	Poisson's ratio	v_c = 0.18	v_c = 0.18
3	Unit weight	24.0 kN/m^3	23.0 kN/m^3

study. The Zirdan RCC dam is one of RCC dam in Iran which is completed and impounded in 2012. It is located in southeast of Iran in 40 kilometers northwest of Pirsohrab village and 60 kilometers north of Chabahar. The crest, length, and reservoir area of this dam are 64 meter, 350 meter, and 16.5 square kilometer, respectively. The initial volume of the reservoir is 217 cubic million meter.

The necessary parameters in analysis process are listed in Table 1. Thereupon, the results of the structural analyses based on Table 1 were used for model verifications.

The RCC gravity dam must endure against various forces that considered in design process. The stability model and accuracy of design is directly related to the kind of discretization of mathematical-numerical model and mesh size in FEM analysis. In this research, the various mesh in FEM process were used and based on error analysis the optimized mesh was selected. The verification of FEMCRTTFD code is performed by statistical comparison of obtained results with reference numerical and experimental data. Fig. 4(a) shows the statistical comparison of FEMCRTTFD with Zou's *et al.* (2017) research.

The results of FEMCRTTFD code verified with shaking table data based on (Wang *et al.,* 2014) research. In this experimental study, the platform size of the shaking table is 3.36 m × 4.86 m and frequency (f) ranges is from 0.1 to 50 Hz. The difference of acceleration record between nonlinear time history analysis (FEMCRTTFD) and shaking table data are shown in Fig. 5(a). Fig. 4(b) shows that there is no significant different between FEMCRTTFD model and the past numerical analysis (RMSE = 0.057 (m), MAE = 0.033 (m), R^2 = 0.99). Fig. 5(b) shows also there is no significant difference with experimental data (RMSE = 1.17 (m/s^2), MAE = 0.068 (m/s^2), R^2 = 0.962).

After validation process Zirdan RCC dam was simulated using

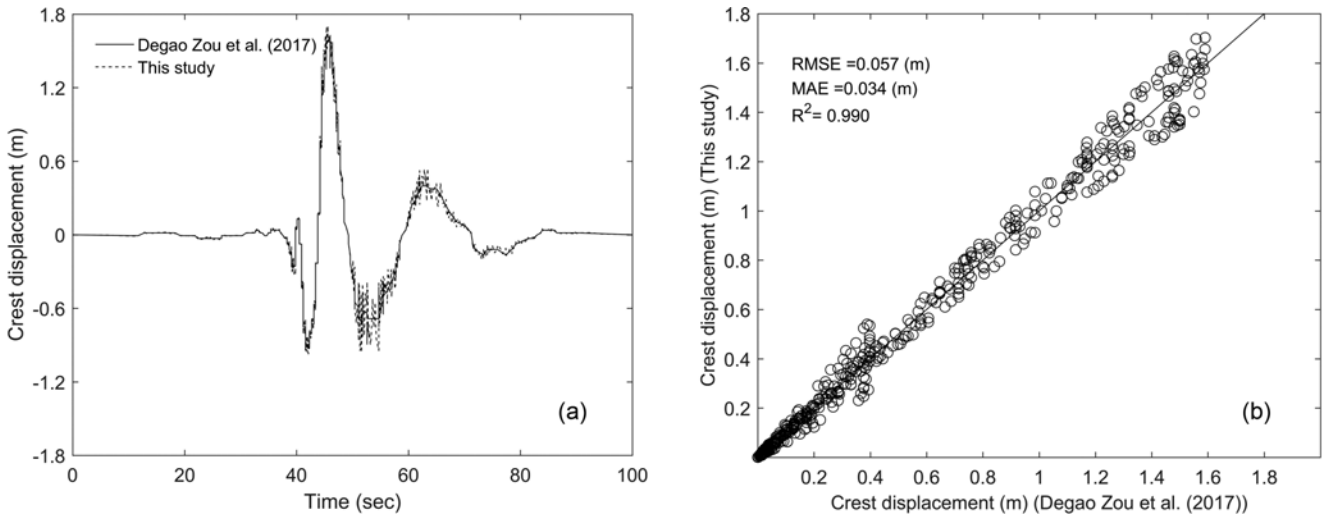

Fig. 4. Verification Graphs: (a) Comparison between This Study and Zou *et al.* (2017) Research, (b) The Statistical Result of Comparison between This Study and Zou *et al.* (2017) Research

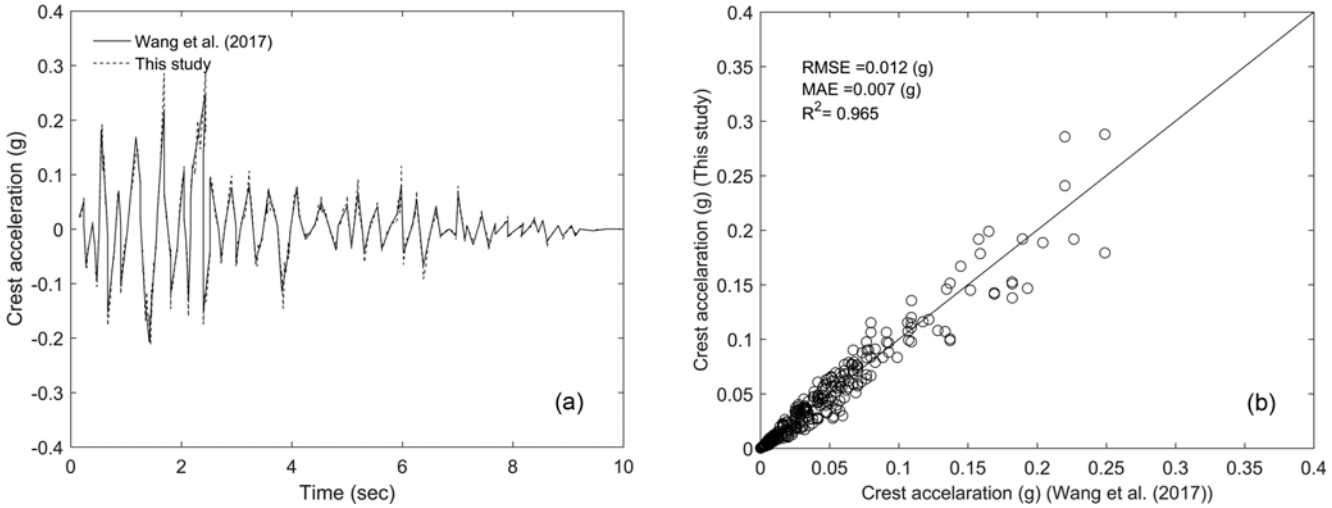

Fig. 5. Verification Graphs: (a) Comparison between This Study and Wang *et al.* (2017) Research, (b) The Statistical Result of Comparison between This Study and Wang *et al.* (2017) Research

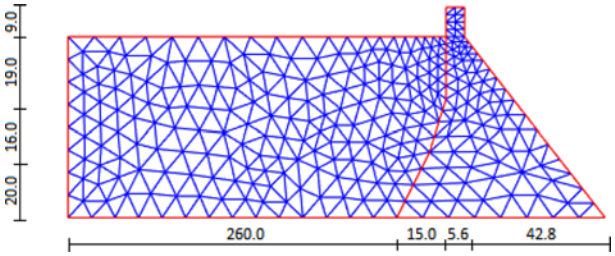

Fig. 6. The Optimized Mesh Size in the FEM Modeling and Dimension of Dam

the validated FEMCRTTFD code. Fig. 6 shows the dimension of main section and the optimized mesh of FEM modeling.

Modal analysis was used to calculate MAC and COMAC matrix. The optimal placement of smart sensors can be find by these matrixes. The combination of the displacement vector of different modes was used to create MAC matrix. Figs. 7, 8, and 9 show the effective mode shape of dam.

5. OSP Process

5.1 COMAC Approach

The modal assurance criterion (MAC) is a mathematical criterion to check the compatibility between two eigenvectors. The MAC is defined as Eq. (7):

$$MAC_{ij} = \frac{(\varphi_i^T \varphi_j)^2}{(\varphi_i^T \varphi_i)(\varphi_j^T \varphi_j)} \tag{7}$$

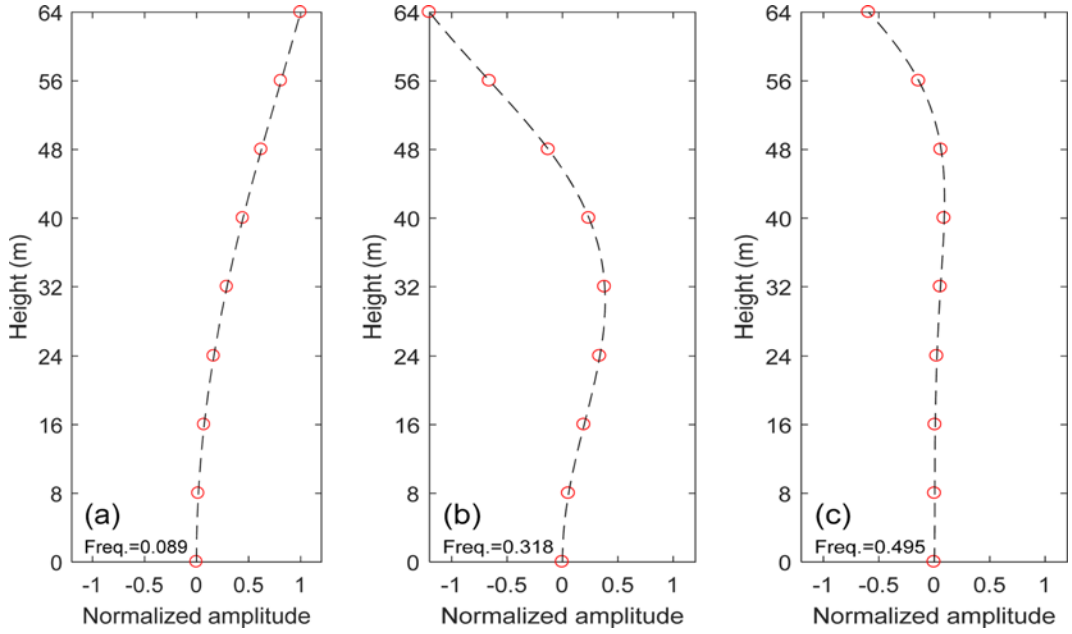

Fig. 7. Identified Natural Frequency and Mode Shape of Zirdan Dam: (a) Mode 1st, (b) Mode 2nd, (c) Mode 3rd

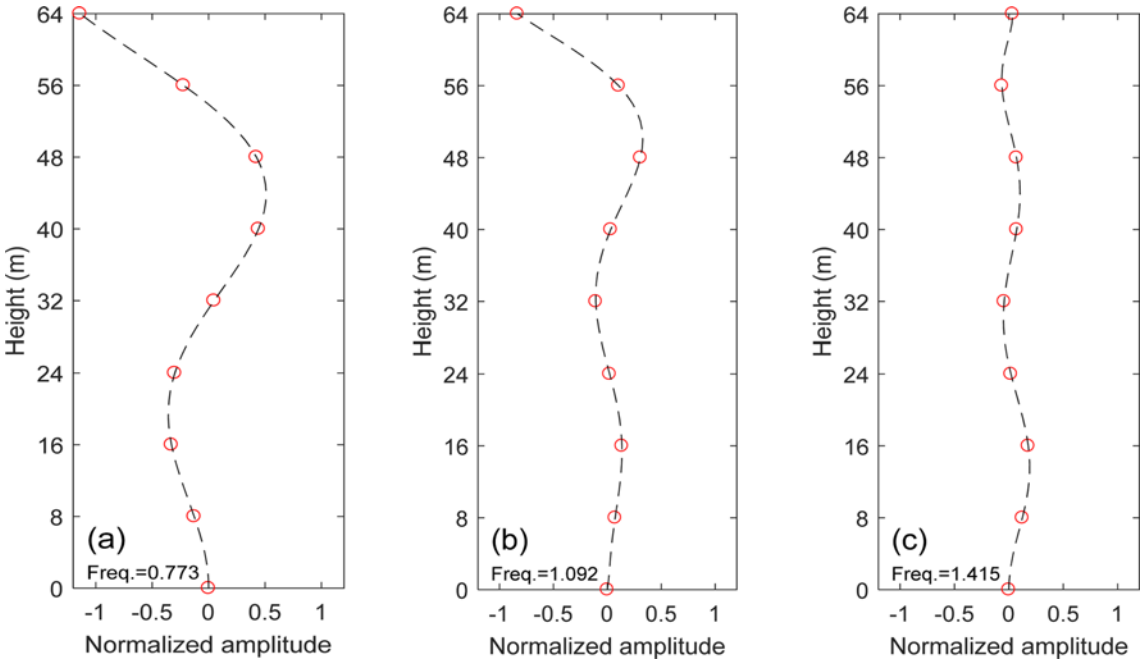

Fig. 8. Identified Natural Frequency and Mode Shape of Zirdan Dam: (a) Mode 4th, (b) Mode 5th, (c) Mode 6th

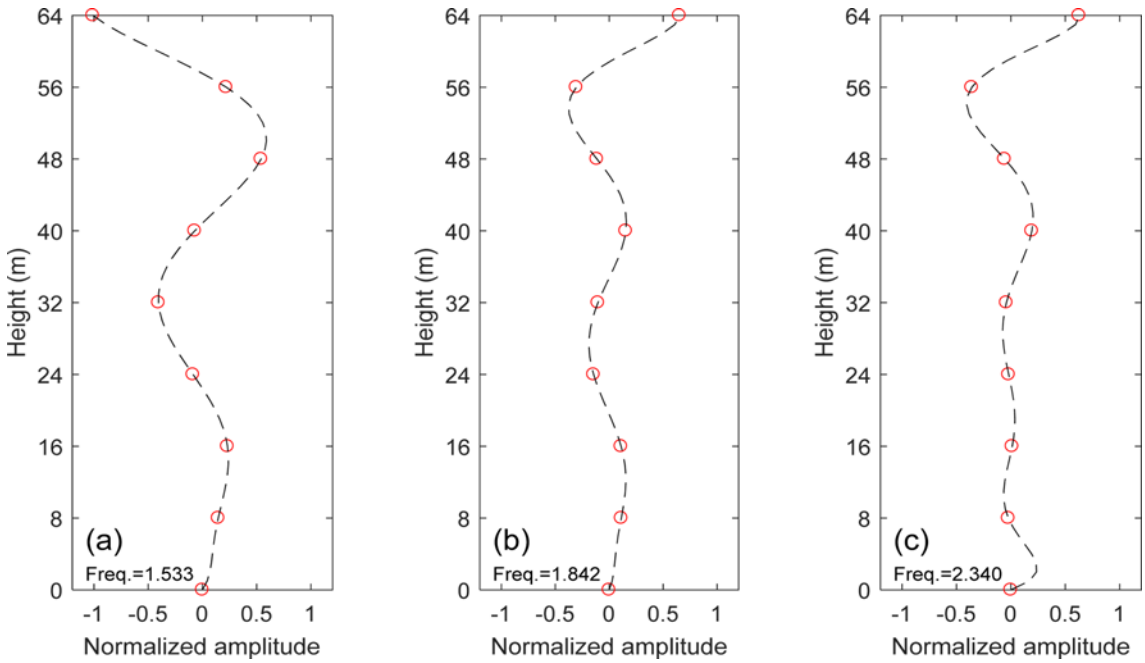

Fig. 9. Identified Natural Frequency and Mode Shape of Zirdan Dam: (a) Mode 7th, (b) Mode 8th, (c) Mode 9th

where φ_i is the eigenvector of mode and i comprising only the measured degrees of freedom. φ_j is the corresponding experimental eigenvector of mode j. In this equation, the MAC values fall within the range between 0 and 1. Zero value of MAC shows lack of any correlation between the off-diagonal element of matrix ($MAC_{ij}(i \neq j)$) and one indicates a high degree of likeness between the modal vectors. The 2D and 3D graphs of MAC value are shown in Fig. 10.

Coordinate modal assurance criterion (COMAC) was developed based on MAC approach. The COMAC approach can identify the placement of smart sensors based on measurement degree-of-freedom with an adverse contribution to the low value of MAC. The COMAC approach is calculated on a set of state pairs such as: Analytical against analytical, experimental against experimental, or analytical versus experimental data. The two modal vectors in each mode pair show the same modal vector, but the set of mode pairs represents all modes of interest within a specific frequency range. A value of COMAC can be computed

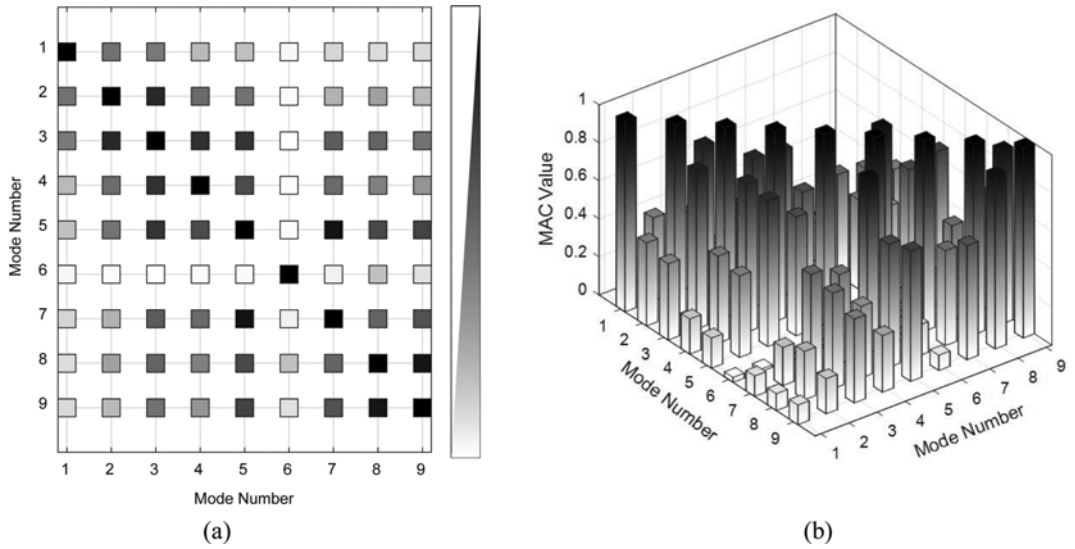

Fig. 10. Plot of MAC Values: (a) 2-D Plot, (b) 3-D Plot

for each degree of freedom to compare both set of conditions. The calculation process of COMAC is defined based on Eq. (8), when the mode pairs have been identified by MAC approach or other proper approach. Ahmet *et al*. (2017) developed this method for cracked area and they evaluated cracked modal shape instead ordinary modal shape:

$$COMAC_{(i)} = \frac{\left|\sum_{j=1}^{m} \varphi_{ij,1}\varphi_{ij,1}\right|^2}{(\sum_{j=1}^{m} \varphi_{ij,1}^2)(\sum_{j=1}^{m} \varphi_{ij,2}^2)} \tag{8}$$

5.2 TTFD (Modified COMAC) Algorithm

Any signal can completely be described in time or frequency domain and so the equivalent periods T_{ei} are obtained. The both representations data in time or frequency domain can transform to each other. This transformation is undertaken by the so-called Fourier transformation and the inverse Fourier transformation are given in Eqs. (9) and (10), respectively:

$$U(\omega) = \int_{-\infty}^{+\infty} u(t).e^{-i\omega t}dt \tag{9}$$

$$u(t) = \frac{1}{2\pi}\int_{-\infty}^{+\infty} U(\omega).e^{i\omega t}d\omega \tag{10}$$

There was no precisely dynamic response on the past presented OSP algorithms, the authors of this paper developed the TTFD algorithm on the basis of non-linear time-history analysis. The mathematical process of TTFD is given by Eq. (11). In first step of this approach, the results of the non-linear analysis were used in order to be obtained the sensors placement exactly. The values of displacement-time output results in time domain must be transformed to frequency-domain in the second step of this approach based on Eq. (10). In the next step of TTFD approach, the effective frequencies according the maximum Fourier amplitude were selected. In step four of this method the normalized seismic displacement of each effective period was considered. In this respect these normalized displacement in Z (j = 1: n) direction act as mode shape in MAC analysis. In this equation n is the number of level of dam that considered to install the FBG sensors. The modified type of COMAC values can be obtained from modified MAC in the last step of this approach:

$$t_i = \begin{Bmatrix} t_1 \\ t_2 \\ t_3 \\ \vdots \\ t_n \end{Bmatrix} \xrightarrow{Step\ 1} u(t)_i = \begin{Bmatrix} u(t)_1 \\ u(t)_2 \\ u(t)_3 \\ \vdots \\ u(t)_n \end{Bmatrix} \xrightarrow{Step\ 2} U(\omega)_i = \begin{Bmatrix} U(\omega)_1 \\ U(\omega)_2 \\ U(\omega)_3 \\ \vdots \\ U(\omega)_n \end{Bmatrix} \xrightarrow{Step\ 3} f_{ei} = \begin{Bmatrix} f_{e1} \\ f_{e2} \\ f_{e3} \\ \vdots \\ f_{en} \end{Bmatrix} \rightarrow T_{ei} = \begin{Bmatrix} T_{e1} \\ T_{e2} \\ T_{e3} \\ \vdots \\ T_{en} \end{Bmatrix}$$

$$T_{ei} = \begin{Bmatrix} T_{e1} \\ T_{e1} \\ T_{e1} \\ \vdots \\ T_{nen} \end{Bmatrix} \xrightarrow{Step\ 4} u(z)_{ei} = \begin{Bmatrix} u_{j(z)e1\ j=1\rightarrow n} \\ u_{j(z)e2\ j=1\rightarrow n} \\ u_{j(z)e3\ j=1\rightarrow n} \\ \vdots \\ u_{j(z)nen\ j=1\rightarrow n} \end{Bmatrix} \&u(x)_{ei} \tag{11}$$

$$= \begin{Bmatrix} u_{j(x)e1\ j=1\rightarrow n} \\ u_{j(x)e2\ j=1\rightarrow n} \\ u_{j(x)e3\ j=1\rightarrow n} \\ \vdots \\ u_{j(x)nen\ j=1\rightarrow n} \end{Bmatrix} \xrightarrow{Step\ 5} \text{Modified COMAC}$$

The complete quadratic combination (CQC) method was utilized as a famous modal combination technique. However, after the time-frequency transformation, the corresponded values of time-history analysis should be substituted with the modal analysis outcomes. Hence, all of the required parameter values in the CQC such as maximum modal responses are replaced with transformed equivalent time histories results.

6. Results

The nonlinear FEM analysis was performed by FEMCRTTFD

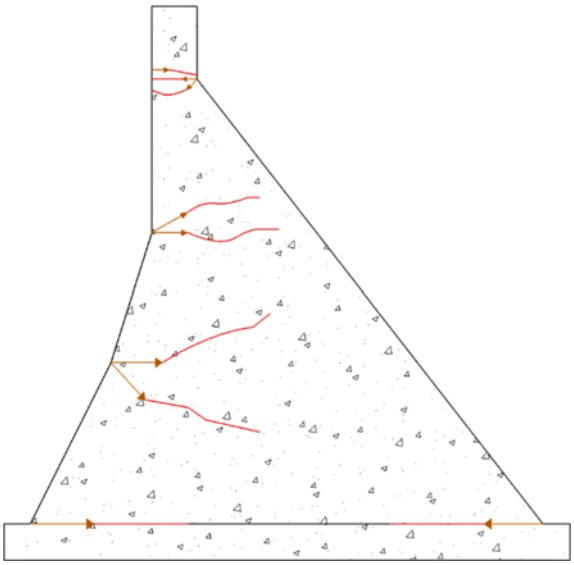

Fig. 11. The Most of Crack and Deep Calculated by FEMCRTTFD Code in the Seismic Analysis Process

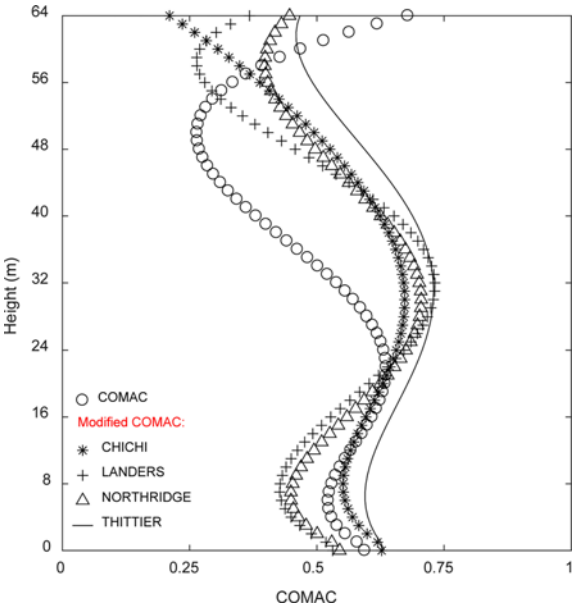

Fig. 12. Results from Comparison of COMAC Diagrams without Seismic Crack with Earthquakes: Chichi, Landers, Northridge, Thittier, in the Far Field

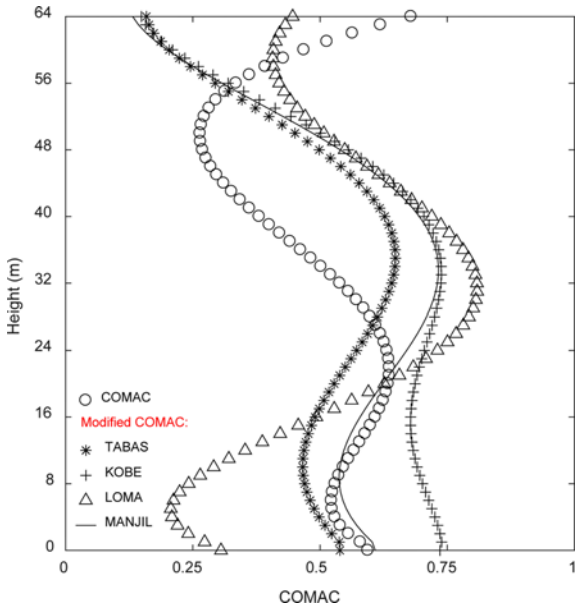

Fig. 13. Results from Comparison of COMAC Diagrams without Seismic Crack with Earthquakes: Tabas, Kobe, Loma, Manjil, in the Near Field

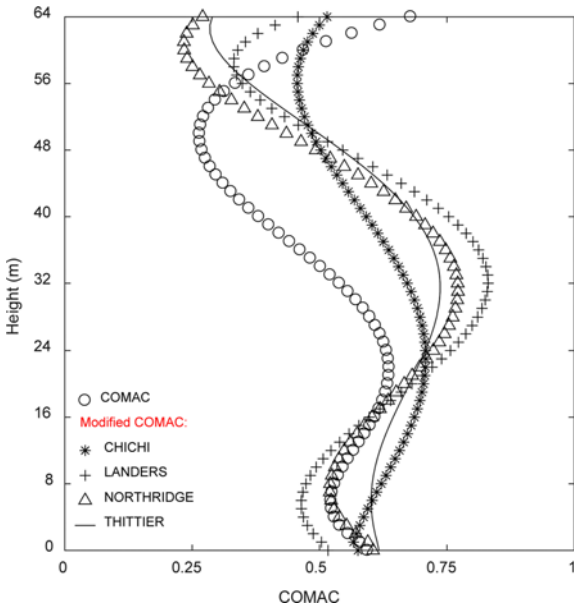

Fig. 14. Results from Comparison of COMAC Diagrams with Seismic Crack with Earthquakes: Chichi, Landers, Northridge, Thittier, in the Far Field

code. The cracks in dam body can be detected using nonlinear time history analysis with set of earthquake ground motions. The six proper earthquake ground motion were selected and scaled to site plan intensity. The results of seismic analysis with FEMCRTTFD show that the potential cracks occur at slope change when seismic loads subject dam from upstream (U/S) to downstream (D/S) face. If the depth of cracks extends in dam body, the seismic damage occurs as sliding or rotational damage. Fig. 11 shows the major cracks of dam's body in near and far field earthquake analysis.

The seismic crack was analyzed by FEMCRTTFD approach and these cracks can be used to optimize sensor location. Regarding TTFD algorithm, the amount of COMAC was calculated according to Eq. (8). Fig. 12 illustrates the comparison between calculation COMAC that calculated by modal analysis with the COMAC that calculated with TTFD method for far-field Chichi, Landers, Northridge and Thittier earthquakes without considering the crack. This figure shows that the OSP of modified COMAC approach in comparison with COMAC method has a good agreement in Landerse earthquake and when the RCC dam was subjected to Thittier seismic waves, there is significant difference with COMAC results. Fig. 13 shows the mentioned amounts for near-

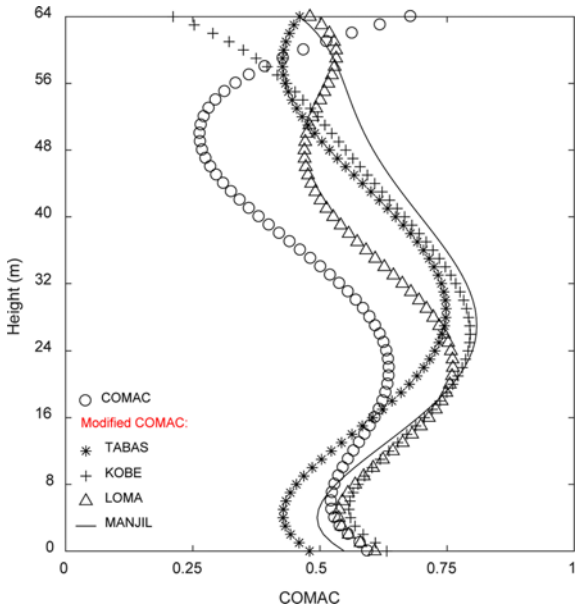

Fig. 15. Results from Comparison of COMAC Diagrams with Seismic Crack with Earthquakes: Tabas, Kobe, Loma, Manjil, in the Near Field

field Kobe, Loma, Tabas, and Manjil earthquakes in without crack condition. The results of this figure show that there are significant difference between calculated sensor placements with dynamic analysis of earthquakes (modified COMAC) with COMAC approach. The mentioned amounts for far-field Chichi, landers, Northridge and Thittier earthquakes with considering the crack effect are shown in Fig. 14. In this figure, the seismic crack was considered in OSP process for the near-field earthquake. According to the figure, the results of Chichi analysis has the most compliance with the modified COMAC results. Fig. 15 shows the mentioned amounts for near-field Kobe, Loma, Tabas, and Manjil earthquakes with considering crack effect. The various analysis of this figure show that there is not any significant difference of OSP calculated between COMAC and modified COMAC approach when RCC dam was subjected to Loma seismic waves. The OSP of dam have good agreement when it were subjected to Kobe and the Manjil earthquakes.

The results show that the proposed approach in this study has good agreement with consideration crack in comparison with the past methods like MAC and COMAC. Fig. 16 illustrates the comparison between COMAC that calculated by modal analysis and TTFD method in without crack mode for far-field Chichi, Landers, Northridge and Thittier earthquakes. The results show that in the far field analyses without considering seismic crack, there are significant differences between all modified COMAC analyses with COMAC approach. Fig. 17 shows the comparison between COMAC calculated by modal analysis and TTFD method in without crack effect for near-field Kobe, Loma, Tabas, and Manjil earthquakes. The results show that in the near field analyses without considering seismic crack, there are significant

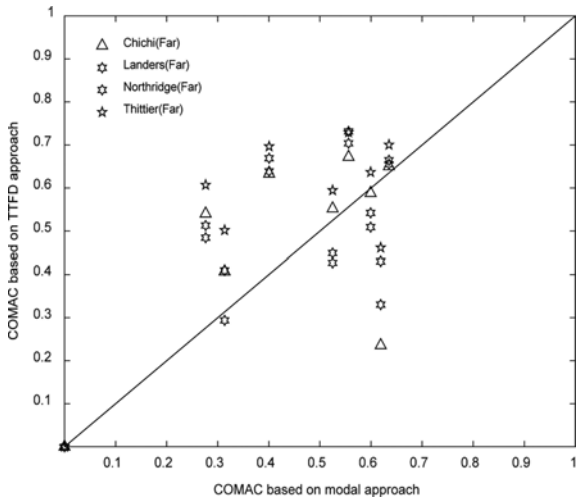

Fig. 16. Comparison between COMAC and Modified COMAC Subjected to Far Filed Earthquake without considering Crack

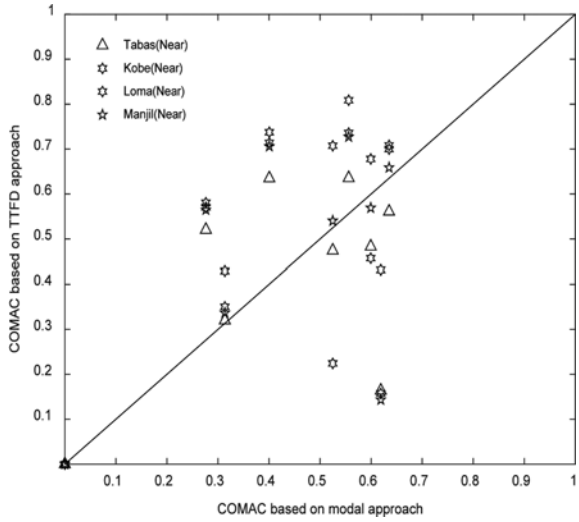

Fig. 17. Comparison between COMAC and Modified COMAC Subjected to Near Filed Earthquake without considering Crack

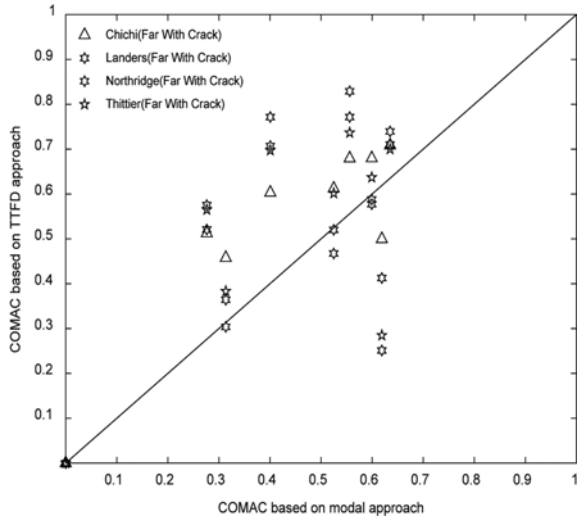

Fig. 18. Comparison between COMAC and Modified COMAC Subjected to Far Filed Earthquake with considering Crack

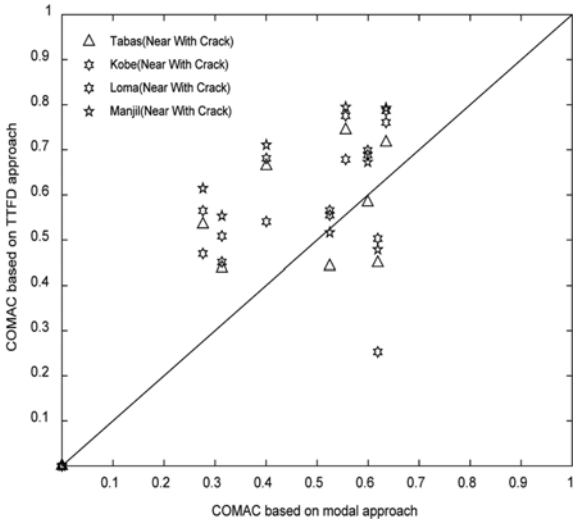

Fig. 19. Comparison between COMAC and Modified COMAC Subjected to Near Filed Earthquake with considering Crack

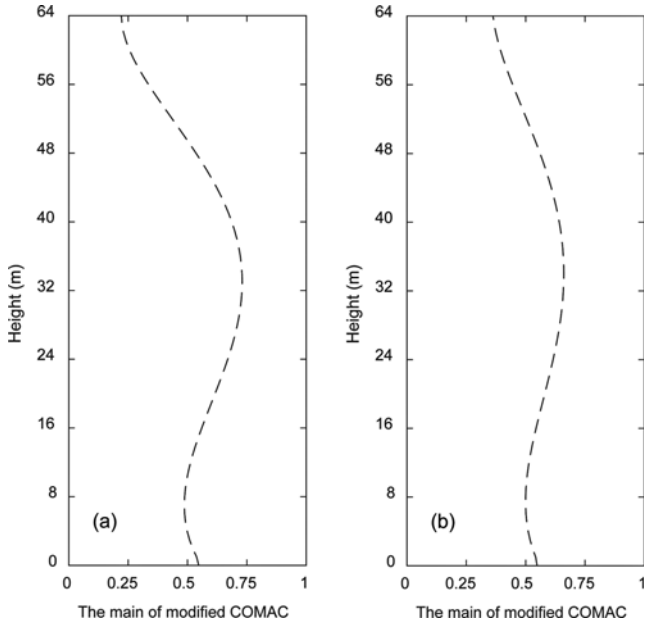

Fig. 20. The Modified COMAC Value based on TTFD Algorithm without Crack Consideration: (a) Near Field Analysis, (b) Far Field Analysis

differences between all modified COMAC analyses with COMAC approach. The amounts with considering cracks, for far-field Chichi, landers, Northridge and Thittier and near-field Kobe, Loma, Tabas, and Manjil earthquakes are shown in Figs. 18 and 19, respectively. In this case, the results are more consistent with the modified COMAC in both the near and far field analyses. In this way the OSP in near field analysis has more good agreement with COMAC approach.

The mean of modified COMAC of analysis dam subjected to near field earthquakes (Tabas, Loma, Kobe, and Manjil) without crack consideration is illustrated in Fig. 20(a). The mentioned value for far field earthquakes without crack consideration is

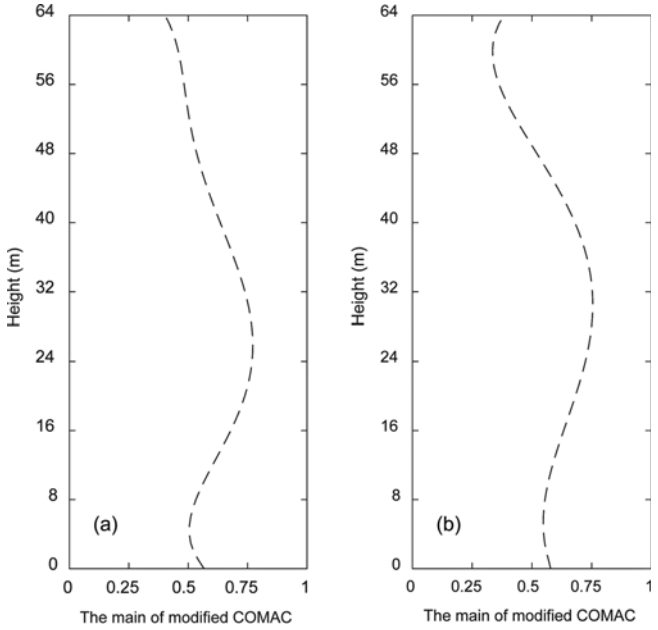

Fig. 21. The Modified COMAC Value based on TTFD Algorithm with Crack Consideration: (a) Near Field Analysis, (b) Far Field Analysis

shown in Fig. 20(b).

In spite of importance the tensile cracks in concert dam, the FEMCRTTFD algorithm can consider cracks in OSP process as a novel approach. Fig. 21(a) shows the mean modified COMAC based on TTFD algorithm in near field earthquakes (Tabas, Loma, Kobe, and Manjil) analysis and the mean modified COMAC for far field earthquakes (Chichi, Landers, Thittier, and Northridge) analysis is shown in Fig. 21(b). The OSP in the dam body without considering crack analysis, can be identifies based on Fig. 20. The OSP process that designed in FEMCRTTFD code can detect the curvature and change of COMAC graph. In this way the OSP of RCC dam was selected with considering the fitness function. The propose approach can consider the amount of COMAC in each analysis to detect the sensor location.

The optimal sensor placement of concrete dam without crack consideration for near and far field analysis based on FEMCRTTFD are shown in Figs. 22(a) and 22(b), respectively. The Figs. 22(c) and 22(d) show the placement of sensors for near and far field earthquake analysis with crack consideration. The OPS by the proposed approach achieves preferable results than other sensor placement cases because based on material described in Fig. 20, The OSP of RCC dam with considering crack analysis can be detected based on Fig. 21. The OSP of RCC dam is shown in Fig. 22.

The statistical results of sensor placement with COMAC criteria in case of COMAC and modified COMAC algorithm without considering any smeared crack is shown in Table 2.

This table indicated that Thittier far-field earthquake has minimum mean absolute error (MAE) and root mean absolute error (RMSE) and maximum R^2 so the modified COMAC and COMAC approach have good agreement on identify optimal

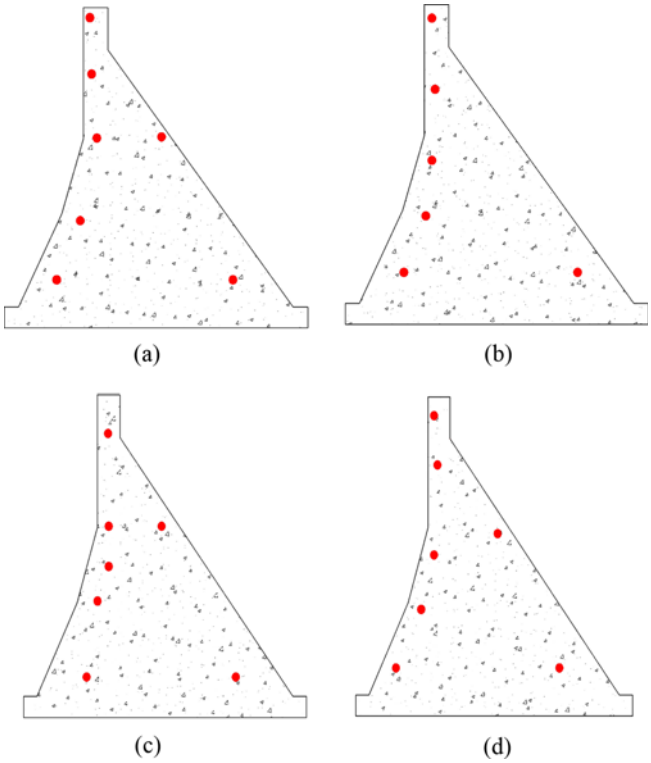

Fig. 22. Optimal Sensor Placement with FEMCRTTFD Approach: (a) Near Filed Analysis without Crack Consideration, (b) Far Field Analysis without Crack Consideration, (c) Near Filed Analysis with Crack Consideration, (d) Far Field Analysis with Crack Consideration

Table 2. The Statistical Comparison between COMAC and Modified COMAC Approach without Crack Consideration

Different approaches	RMSE	MAE	Correlation coefficient (R^2)	p-value
Tabas near field	0.187	0.159	0.912	0.630
Kobe near field	0.142	0.106	0.835	0.666
Loma near field	0.173	0.128	0.595	0.387
Manjil near field	0.171	0.139	0.814	0.340
Chichi far field	0.137	0.115	0.903	0.190
Landers far field	0.179	0.125	0.660	0.222
Northridge far field	0.142	0.102	0.665	0.297
Thittier far field	0.071	0.056	0.856	0.605

sensor placement. A similar reduction was seen in MAE and RMSE by using TTFD instead of existing equations. Fig. 23 shows that the periods with maximum Fourier amplitude is very close to natural periods of structure when the results of time domain analysis transferred to frequency domain. This figure also shows in this condition the sensors placement in modified COMAC and COMAC have a proper adaptively. It can be showed for far-field Chichi earthquake which is illustrated in Fig. 24. Statistically analysis using SPSS code based on independent Mann-Whitney test show that there is no significant difference between the placement of sensors that identified by modified COMAC and COMAC (the mean p-value = 0.449 > 0.05).

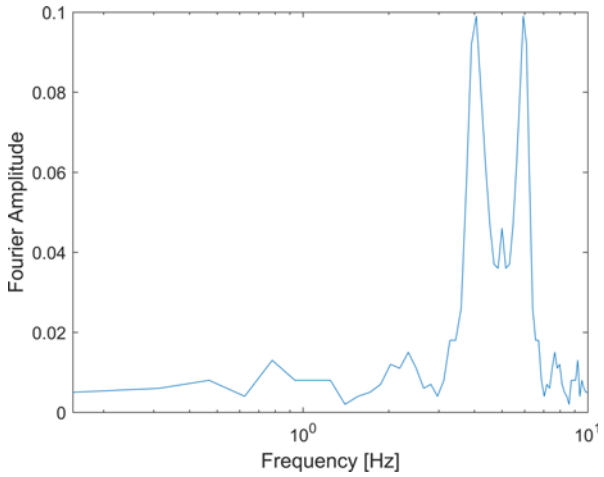

Fig. 23. Frequency Fourier Amplitude for Far Field Earthquake Thittier without considering Crack

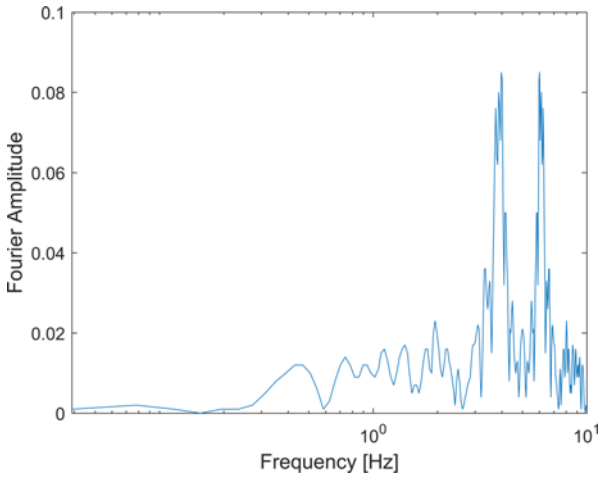

Fig. 24. Frequency Fourier Amplitude for Near Field Earthquake Chichi without considering Crack

The statistical analysis show that COMAC method calculated by modal analysis according to COMAC theory, cannot identify the exact location of smart sensors, but modified COMAC method considers dam structure behavior in far-field and near-field earthquakes so with this approach the optimal sensor location can be detected. The results show that in some earthquakes, considering non- linear time history and transferred results to frequency domain and COMAC calculation based on this transferring has an acceptable accuracy on identify the sensor location. In some cases, the calculated amount is closer to the amount calculated by modal algorithm and this is due to the earthquake frequency content. So this method can assess the exact location of optimized smart sensors. The proposed method in this study can identify location of smart sensors regarding based on actual seismic behavior of structure. The results of the analysis to optimize location of sensors are dependent on seismic analysis according to seismic records. Therefore, the optimal sensors placement is determined regarding the real behavior of dam that were subjected to far or near field earthquake. The

Table 3. The Statistical Comparison between MODAL and TTFD Approach with Crack Consideration

Different approaches	RMSE	MAE	Correlation coefficient (R^2)	p-value
Tabas near field	0.176	0.145	0.622	1.000
Kobe near field	0.106	0.077	0.923	0.489
Loma near field	0.178	0.132	0.635	0.796
Manjil near field	0.182	0.144	0.752	0.340
Chichi far field	0.199	0.156	0.513	0.605
Landers far field	0.141	0.105	0.825	0.666
Northridge far field	0.071	0.053	0.953	0.796
Thittier far field	0.097	0.075	0.931	0.666

statistical analysis results between COMAC that calculated by modern modified COMAC algorithm are given in Table 3.

The statistical analysis show that COMAC method calculated by modal analysis according to COMAC theory, cannot identify the exact location of smart sensors, but modified COMAC method considers dam structure behavior in far-field and near-field earthquakes so with this approach the optimal sensor location can be detected. The results show that in some earthquakes, considering non-linear time history and transferred results to frequency domain and COMAC calculation based on this transferring has an acceptable accuracy on identify the sensor location. In some cases, the calculated amount is closer to the amount calculated by modal algorithm and this is due to the earthquake frequency content. So this method can assess the exact location of optimized smart sensors. The proposed method in this study can identify location of smart sensors regarding based on actual seismic behavior of structure. The results of the analysis to optimize location of sensors are dependent on seismic analysis according to seismic records. Therefore, the optimal sensors placement is determined regarding the real behavior of dam that were subjected to far or near field earthquake. The statistical analysis results between COMAC that calculated by modern modified COMAC algorithm are given in Table 3.

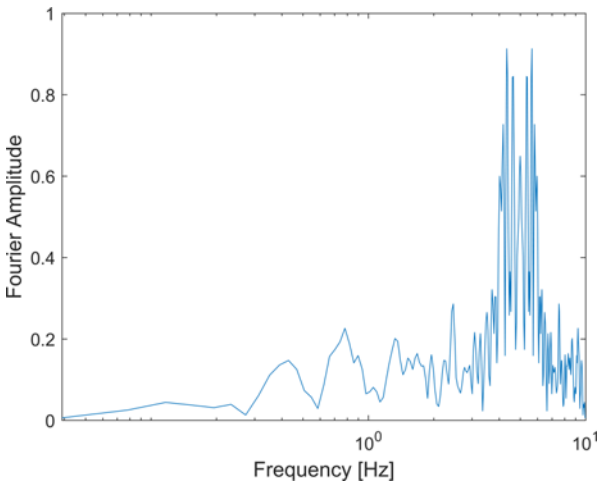

Fig. 25. Frequency Fourier Amplitude for Far Field Earthquake Chichi with Crack

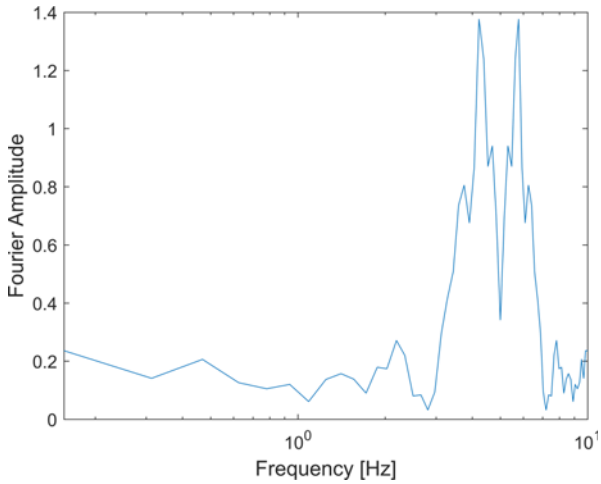

Fig. 26. Frequency Fourier Amplitude for Near Field Earthquake Thittier with Crack

These results show, the COMAC amounts based on far-field Northridge earthquake is in more agreement with the same amounts that calculated by modal analysis. Kobe, far-field earthquake is also in agreement with the amounts that calculated by modal analysis too. From another view, identification optimal placement of sensors based on far-field earthquake has maximum R^2 and minimum MAE and RMSE in comparison with COMAC approach than near field earthquake. There is significant difference between Chichi far-field earthquakes with modal analysis based on COMAC approach. The reason of this difference can be found in Fig. 25 that there is poor agreement between frequencies with maximum magnitude with modal analysis in frequency domain. It can be showed for near-field Thittier earthquake which is illustrated in Fig. 26. Statistically analysis using SPSS code based on independent Mann-Whitney test show that there is no significant difference between the placement of sensors that identified by modified COMAC and COMAC (the mean p-value = 0.717 > 0.05).

7. Conclusions

The present study is the first to introduce a novel based approach for optimal sensor placement of concrete dams. The main advantage of proposed approach is to characterize the nonlinear dynamics due to seismic-impacts with a view toward SHM and damage detection of dams. This technique was designed and developed by nonlinear time history analysis and modified COMAC approach with transferring time history results to frequency domain. The optimal sensors were placed to maintain the dynamically analysis information in the frequency domain base on time history response of dam and the overall system displacement within the frequency range of interest. The frequency domain OSP technique that proposed in this research can be used for all effective frequency ranges of dam. The novel sensor placement strategy is first utilized to determine the optimal sensor layout based on COMAC approach with limited

number of sensors placed on a dam. In fact, the modified COMAC approach brings about significant performance improvements with changes in the COMAC approach to enable optimal method in OSP process. The accuracy of this method was validated through by comparing the model output to reference research and validation results show that there is good agreement between them. The effectiveness of the sensor placement by the proposed method is successfully verified by comparison. The proposed method can be employed in any concrete RCC dam and even in other hydraulic structure for health monitoring.

References

Altunışık, A. C., Okur, F. Y., and Kahya, V. (2017). "Modal parameter identification and vibration based damage detection of a multiple cracked cantilever beam." *Journal of Engineering Failure Analysis*, Vol. 79, pp. 154-170, DOI: 10.1016/j.engfailanal.2017.04.026.

Bazant, Z. P. and Tabbara, M. R. (1990). "Random particle models for fracture of aggregate or fiber composites." *Journal of Engineering Mechanics,* Vol. 116, No. 8, pp. 1686-1705, DOI: 10.1061/(ASCE) 0733-9399(1990)116:8(1686).

Guo H. Y., Zhang, L., Zhang, L. L., and Zhou, J. X. (2004). "Optimal placement of sensors for structural health monitoring using improved genetic algorithms." *Smart Materials and Structures,* Vol. 13, No. 3, pp. 528-534, DOI: DOI: 10.1088/0964-1726/13/3/011.

Hariri-Ardebili, M. A. and Seyed-Kolbadi, S. M. (2015). "Seismic cracking and instability of concrete dams: Smeared crack approach." *Journal of Engineering Failure Analysis*, Vol. 52, pp. 45-60, DOI: 10.1016/j.engfailanal.2015.02.020.

Harris, D. W., Snorteland, N., Dolen, T., and Travers, F. (2000). "Shaking table 2-D models of a concrete gravity dam." *Earthquake Engineering Structure Dynamics*, Vol. 9, No. 6, pp. 769-787, DOI: 10.1002/(SICI)1096-9845(200006)29:6<769::AID-EQE925>3.0.CO; 2-7.

Hemez, F. M. and Farhat, C. (1994). "An energy based optimum sensor placement criterion and its application to structure damage detection." *Proc. 12th Conference on International Modal Analysis*, Honolulu, HI, USA, pp. 1568-1575.

Hillerborg A., Modeer, M., and Petersson, P. E. (1976). "Analysis of crack formation and crack growth in concrete by means of fracture mechanics and finite elements." *Cement and Concrete Research,* Vol. 6, No. 6, pp. 773-781, DOI: 10.1016/0008-8846(76)90007-7.

Hiramoto, K., Doki, H., and Obinata, G. (2000). "Optimal sensor actuator placement for active vibration control using explicit solution of algebraic Riccati equation." *Journal of Sound and Vibration*, Vol. 229, No. 5, pp. 1057-1075, DOI: 10.1006/jsvi.1999.2530.

Huang Z., Shen, X., and Tang, C. (2008). "Numerical simulation of instability failure of high rolled compacted concrete gravity dam." *Journal of Shenyang University Technology*, Vol. 30, No. 5, pp 591-594.

Javanmardi, F., Leger, P., and Tinawi, R. (2005). "Seismic structural stability of concrete gravity dams considering transient uplift pressures in cracks." *Engineer Structure*, Vol. 27, No. 4, pp. 616-28, DOI: 10.1016/j.engstruct. 2004.12.005.

Ju, M., Park, C., and Kim, G. (2015). "Structural Health Monitoring (SHM) for a cable stayed bridge under typhoon." *KSCE Journal of Civil Engineering*, Vol. 19, No. 4, pp. 1058-1068, DOI: 10.1007/ s12205-015-0039-3.

Mohamed, A. R. and Hansen, W. (1999). "Micromechanical modeling of concrete response under static loading. Part I: Model development and validation." *ACI Mater Journal,* Vol 96, No. 2, pp. 196-203.

Moradi, M., Vosoughifar, H., and Hassanzadeh, Y. (2014). "Optimal placement of smart sensors in the underground storage tanks regarding to the cavitation effect by Monte Carlo analysis." *Proc. 2nd International Congress on Structure*, Tabriz Islamic Art University, Tabriz, Iran.

Rashid, Y. R. (1968). "Ultimate strength analysis of prestressed concrete pressure vessels." *Nuclear Engineering and Design*, Vol. 7, No. 4, pp. 334-344, DOI: 10.1016/0029-5493(68)90066-6.

Rathi, S. and Gupta, R. (2016). "A simple sensor placement approach for regular monitoring and contamination detection in water distribution networks." *KSCE Journal of Civil Engineering,* Vol. 20, No. 2, pp. 597-608, DOI: 10.1007/s12205-015-0024-x.

Saini, S. S., Krishna, J., and Chandrasekaran, A. (1972). "Behavior of Koyna Dam—Dec. 11, 1967 earthquake." *Journal of the Structural Division*, Vol. 98, No. 7, pp. 1395-1412.

Schlangen, E. and Garboczi, E. J. (1997). "Fracture simulations of concrete using lattice models: Computational aspects." *Engineering Fracture Mechanics*, Vol. 57, Nos. 2-3, pp. 319-332, DOI: 10.1016/ S0013-7944(97)00010-6.

Shi, Z. Y., Law, S. S., and Zhang, L. M. (2000). "Optimum sensor placement for structural damage detection." *J. Eng. Mech*., Vol. 126, No. 11, DOI: 10.1061/(ASCE)0733-9399(2000)126:11(1173).

Shokouhi, S. K. S., Dolatshah, A., Vosoughifar, H., Rahnavard, Y., and Dowlatshahi, B. (2013). "Optimal sensor placement in the Base-Isolated structures subjected to near-fault earthquakes using a novel TTFD approach." *Sensors and Smart Structures Technologies for Civil, Mechanical, and Aerospace Systems,* Vol. 8692, pp. 900-924, DOI: 10.1117/12.2012010.

Tang, C. A. and Zhu, W. C. (2003). *Damage and fracture of concrete numerical simulation,* Science Press, Beijing, China, pp. 120-145.

Vosoughifar, H. and Shokouhi, S. K. S. (2013). "Health monitoring of LSF structure via novel TTFD approach." *Civil Structural Health Monitoring Workshop (CSHM-4),* Berlin, Germany.

Vosoughifar, H., Shokouhi, S. K. S., and Farshadmanesh, P. (2012). "Optimal sensor placement of steel Structure with UBF system for SHM using hybrid FEM-GA technique." *Civil Structural Health Monitoring Workshop (CSHM-4),* Berlin, Germany.

Wang, Z., Liu, S., Vallejo, L., and Wang, L. (2014). "Numerical analysis of the causes of face slab cracks in Gongboxia rockfill dam." *Engineering Geology*, Vol. 181, pp. 224-232, DOI: 10.1016/j.enggeo. 2014.07.019.

Wang, G., Wang, Y., Lu, W., Yu, M., and Wang, C. (2017). "Deterministic 3D seismic damage analysis of Guandi concrete gravity dam: A case study." *J. Engineering Structures,* Vol. 148, pp. 263-276, DOI: 10.1016/j.engstruct.2017.06.060.

Wang, J., Yang, G., Liu, H., Nimbalkar, S. S., Tang, X., and Xiao, Y. (2017). "Seismic response of concrete-rockfill combination dam using large-scale shaking table tests." *Soil Dynamics and Earthquake Engineering*, Vol. 99, pp. 9-19, DOI: 10.1016/j.soildyn. 2017.04.015.

Worden, K. and Burrows, A. P. (2001). "Optimal sensor placement for fault detection." *Engineer Structure,* Vol. 23, No. 8, pp. 885-901, DOI: 10.1016/S0141-0296(00)00118-8.

Wouwer, A. V., Point, N., Porteman, S., and Remy, M. (2000). "An approach to the selection of optimal sensor locations in distributed parameter systems." *Journal of Process Control*, Vol. 10, No. 4, pp. 291-300, DOI: 10.1016/S0959-1524(99)00048-7.

Xiong, K., Hua, J., and Li, R. (2014). "Static and seismic failure modes

and structural safety of Oyuk Dam considering material heterogeneity." *Journal of Yangtze River Scientific Research Institute,* Vol. 31, No. 7, pp. 74-80.

Zhang, C. H., Pan, J., and Wang, J. (2009). "Influence of seismic input mechanisms and radiation damping on arch dam response." *Soil Dynamics and Earthquake Engineering*, Vol. 29, No. 9, pp. 1282-1293, DOI: 10.1016/j.soildyn.2009.03.003.

Zhao, J., Bao, T., and Amjad, U. (2015). "Optical fiber sensing of small cracks in isotropic homogeneous materials." *Journal Sensors and Actuators A: Physical,* Vol. 225, pp. 133-138, DOI: 10.1016/j.sna.2015.02.017.

Zhong, H., Lin, G., and Li, H. (2009). "Numerical simulation of damage in high arch dam due to earthquake." *Frontiers of Architecture and Civil Engineering in China*, Vol. 3, No. 3, pp. 316-322, DOI: 10.1007/s11709-009-0039-9.

Zhu, X. Y. and Pekau, O. A. (2007). "Seismic behavior of concrete gravity dams with penetrated cracks and equivalent impact damping." *Engineering Structures,* Vol. 29, No. 3, pp. 336-345, DOI: 10.1016/j.engstruct.2006.05.002.

Zou, D., Han, H., Liu, J., Yang, D., and Kong, X. (2017). "Seismic failure analysis for a high concrete face rockfill dam subjected to near-fault pulse-like ground motions." *Soil Dynamics and Earthquake Engineering*, Vol. 98, pp. 235-243, DOI: 10.1016/j.soildyn.2017.03.031.